RSC Advances

ROYAL SOCIETY OF CHEMISTRY

www.rsc.org/advances

Journal Name

COMMUNICATION

Visible light-induced Photocatalytic Activity of High Surface Area N-doped Two-dimensional (2-D) TiO_2 Sheets

Received 00th January 20xx,
Accepted 00th January 20xx

DOI: 10.1039/x0xx00000x

www.rsc.org/

A. Nikhil, G. S. Anjusree, Shantikumar V Nair and A. Sreekumaran Nair*

TiO_2 being a wide band-gap material offers photocatalytic activity only in the UV region. The effects of simultaneously improving the surface area and nitrogen doping on the visible light–assisted photocatalytic activity of titanate-derived two-dimensional 2-D sheets of TiO_2 has been investigated. Results indicate a remarkable efficiency in the photocatalytic degradation of methyl orange in aqueous environment when compared to undoped 2-D TiO_2 sheets.

The semiconductor photocatalysis have drawn much attention over the past few decades due to its desirable electronic structure, light absorption properties, charge transport characteristics and excitions life time[1]. Among the many players[2], TiO_2 has been widely investigated for its non-toxicity, inexpensiveness, good stability under illumination in most environments and desired surface chemistry[3]. As a result, it is also been used for application in solar energy conversion[4], photodegradation of organic pollutants in water[5], self-cleaning coatings[6], storage devices (supercapacitors and batteries), and sensors[7]. Various morphologies of TiO_2 have been widely explored for photocatalysis such as nanoparticles (zero-dimensional, 0-D) and 1-D nanostructures such as nanofibers, wires and nanorods[8a,b,c].Though the 1-D nanostructures have several merits such as strong light scattering, semi-directional electron transport and higher electron diffusion coefficient, they suffer from low internal surface area which might affect the effective adsorption of contaminants on the surface of the TiO_2 and hence the photocatalytic degradation efficiency. An in-depth investigation of the literature presented to us the prospects of adopting the titanate route for enhancing the surface area of TiO_2[9a,b]. Titanate route is one of the versatile methods for improving the surface area of TiO_2 under the action of NaOH. Compared to 1-D nanostructures[10,11,12],2-D nanostructures would have better surface area (because of their layered nature) but very few reports exist on 2-D nanostructures of TiO_2 for photocatalysis[13,14,15].Th mechanism of photocatalysis by TiO_2 is relatively well established:TiO_2 being a wide band-gap material, absorbs U radiation from the light source and produces pair of electrons and holes. The electrons react with oxygen molecules to form super oxide anions and the positive holes react with the water molecules to form hydrogen molecules and hydroxyl radicals. These hydroxyl radicals (●OH) play a major role in degrading the pollutant by photocatalytic oxidation reaction. Also, it is reported that the formation rate of ●OH is higher in anatase TiO_2 when compared to other semiconductors[16,17]. However, TiO_2 can show photoactivity only in the UV region (absorption onset at 380 nm) which accounts only for ~4% of the solar spectrum and thus the photocatalytic efficiency with pure TiO_2 will be low. A fascinating method by which the absorption spectrum of TiO_2 can be shifted from UV to visible region doping. Doping of metals[18,19,20,21],non-metals[22,23,24,25]and Co doping[26,27]with two or more metals or non-metals is an effective way of promoting absorption of visible light photons (~ 46% of the solar spectrum)and this methodology also provides the pathway for reducing the electron-hole recombination as reported in the literature[28].

Electrospinning technique is one of the most commercially viable techniques for fabricating 1-D structures such as nanowires, nanotubes, nanorods, nanofibers[29a,b] etc. However, as mentioned previously in the introduction, the electrospun 1-D nanostructures suffer from low internal surface areas and hence their photocatalytic efficiency is limited. We have adopted the titanate route to restructure the 1-D TiO_2 into 2-D TiO_2 which takes care of the surface area issue. The 1-D TiO_2–SiO_2 composite obtained from electrospinning was converte into 2-D TiO_2 by the titanate route which involves in-situ etching of SiO_2 and as well as chemically transforming the 1-D TiO_2 into $Na_2Ti_3O_7$ (a layered material) further subseque conversion of the $Na_2Ti_3O_7$ into TiO_2 by retaining th morphology as that of the $Na_2Ti_3O_7$ was obtained b acidification and low temperature sintering (180 °C). Urea w used as the N source during the electrospinning

Amrita Centre for Nanosciences & Molecular Medicine, Amrita Institute of Medical Science, AIMS PO, Ponekkara, Kochi 682041, Kerala, India. E-mail: sreekumarannair@aims.amrita.edu
† Electronic Supplementary Information (ESI) available: characterization details
DOI: 10.1039/x0xx00000x

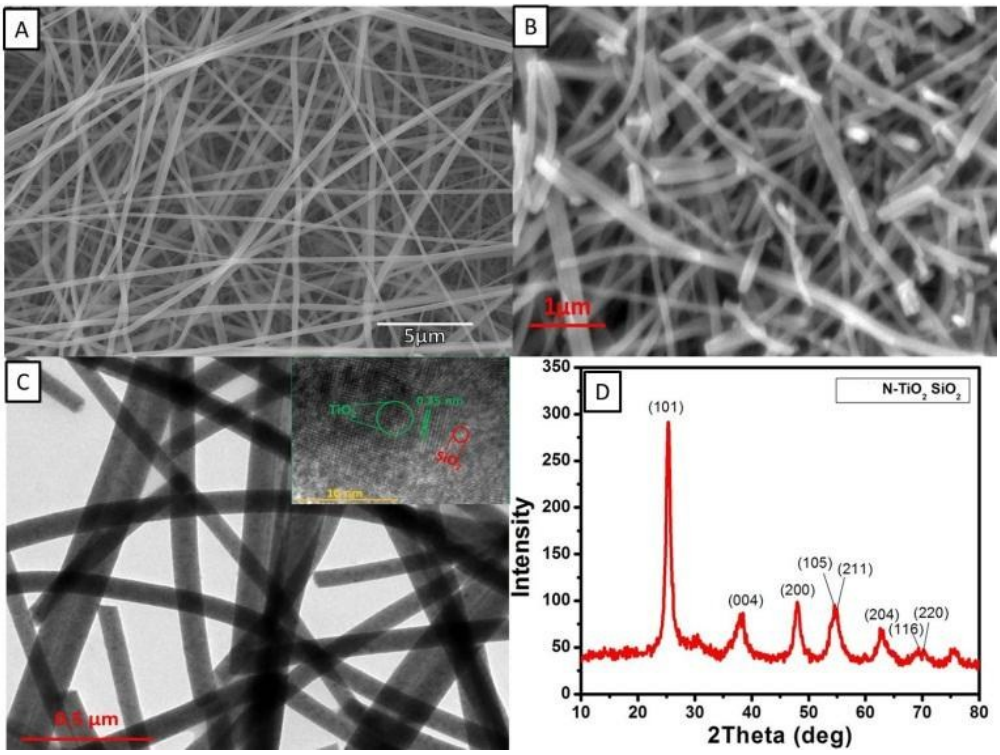

Fig. 1 (A) As-spun N-TiO_2-SiO_2-PVP composite fibers (B) N-TiO_2-SiO_2fibers formed after annealing at 450 ^oC (C) Lattice resolved TEM image of N-TiO_2-SiO_2 composite (D) XRD spectra of N-TiO_2- SiO_2 composite.

process to ensure N doping on the TiO_2 2-D sheets. Thus in the present work we report a facile method to synthesize 2-D TiO_2nanosheets via titanate route along with N doping which has the combined effect of both high surface area and enhanced absorption in the visible region. A comparison of the photocatalytic activity of the N-doped 2-D sheets with un-doped 2-D sheets has shown that N doped 2-D TiO_2 sheets showed superior photocatalytic activity in the visible region.

The powder XRD was performed by an X'pert pro PAN Analytical instrument operated at a current of 30 mA and a voltage of 40 kV (the data interval was 0.03^o). The scanning electron Microscopy was performed by JSM 6490 LA (JEOL-Tokyo, Japan) machine at an operating voltage of 15 kV. A thin film of gold was sputtered on the samples using a sputter coating machine (JEOL-Tokyo, Japan). Raman spectroscopy was done using a Witec Confocal Raman-300 AR instrument with an excitation laser of 488 nm and a power of 0.6 μW. UV-visible spectra of the thin films of TiO_2 (in diffuse-reflectance mode) were measured by a Varian-Cary 5000 spectrometer and UV-visible absorption spectra of the methyl orange were measured using a UV-1800 Shimadzu double beam spectrophotometer. High-resolution Transmission Electron Microscopy (HR-TEM) (SEI Tecnai G230) was also carried out for characterizing the materials. The photocatalytic activity was measured under an illumination of 1 Sun (AM 1.5G) using a solar simulator (Newport, Oriel class A).

The N-doped TiO_2fibers were prepared as follows: A solution was made by dissolving 1 g of PVP (polyvinylpyrrolidone) and 0.07 g of Urea (7 wt. %) in 14mL methanol (Aldrich). The solution was stirred for 12 h followed by the addition of 4 mL acetic acid, 1.75 mL of titanium (IV) isopropoxide (Aldrich) and 0.25 mL of tetraethoxysilane (Alfa Aesar). The solution was electrospun using a climate-controlled electrospinning unit (IME technologies, Netherlands) maintaining the humidity level at ~ 50% inside the electrospinning chamber. The operating conditions were a voltage of 25 kV and a flow-rate of 1 mL/h. The distance between the needle-tip and the static collector was kept at about 15 cm and the as-spun nanocomposite (N-TiO_2-SiO_2-PVP) was collected in the aluminium foil wrapped on the static collector. In order to degrade the polymer, the composite was annealed at 450 ^oC for 3 h resulting in the formation of white flakes. About 600 mg of the annealed N-TiO_2-SiO_2 composite nanofibers were treated with 5M NaOH (in water) at 180 ^oC for 24 h in a Teflon-lined steel autoclave to chemically convert the nanocomposite into titanates with the in-situ etching of SiO_2. A fluffy white precipitate obtained as a result of the chemical reaction was washed repeatedly with Millipore water to neutralise the pH to 7. The sodium titanate was then treated with dil. HCl (0.1 M ACS, ISO Reag.) for 24 h and further washed repeatedly with Millipore water and dried at 180 ^oC for 30 min. The drying process was carried out to convert the sodium titanate into N-TiO_2 through hydrogen titanate. The $Na_2Ti_3O_7$ and the final TiO_2 were characterized by spectroscopy and microscopy, respectively.

Fig. 1A shows the SEM image of as-spun N-TiO_2-SiO_2-PVP fibers which were found to be smooth and continuous with

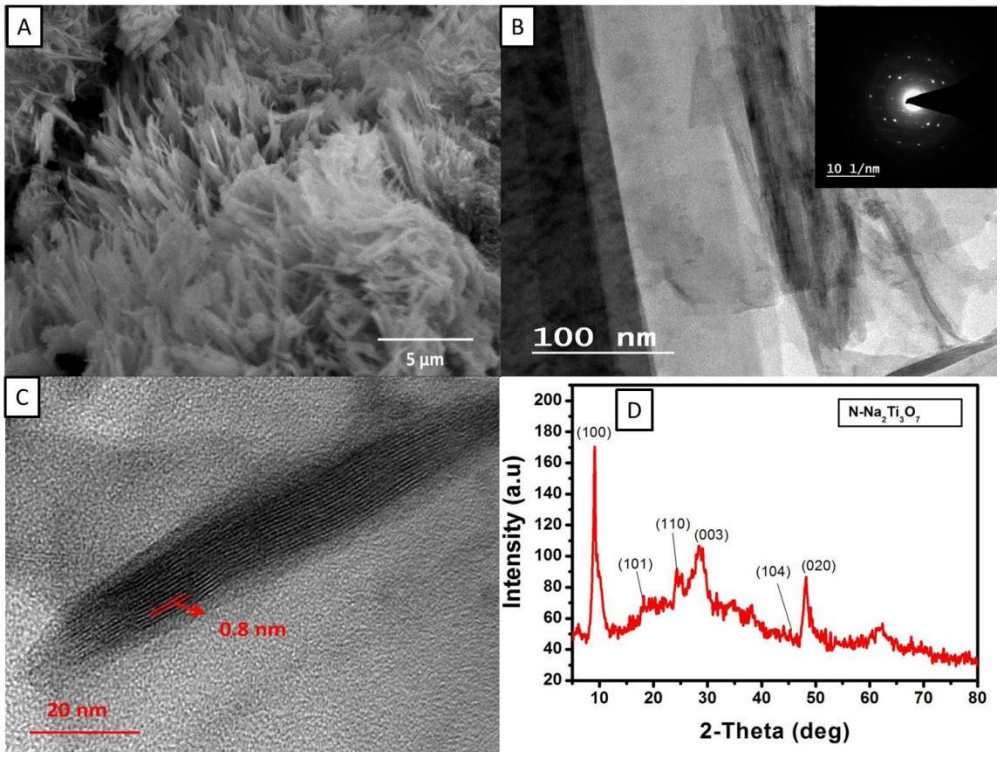

Fig. 2 (A) SEM image of sheet-like structure of N-$Na_2Ti_3O_7$ (B) TEM image of sheet- like structure of N-$Na_2Ti_3O_7$ (C) Lattice-resolved TEM image of N-$Na_2Ti_3O_7$ (D) XRD spectra of N-$Na_2Ti_3O_7$.

diameters ranging from 140-260 nm. Fig. 1B indicates the sintered nanofibers at 450 ^oC (for 3h) having diameter ranging from 93-124 nm. The decrease in the fiber diameter is due to the polymer degradation. Also it is evident from Fig. 1B that the introduction of SiO_2 into the TiO_2 matrix resulted in some of the nanofibers losing their continuous fiber morphology. Fig. 1C shows the lattice-resolved TEM image of TiO_2-SiO_2 composite indicating the TiO_2 fringes corresponding to 0.35 nm implying the anatase nature of TiO_2.The lattice corresponding to SiO_2 was absent which depicts its amorphous nature which is further evident from the powder XRD spectrum showing the prominent peaks of anatase TiO_2[30] alone (Fig. 1D). Elemental mapping was carried out using EDS and the presence of N, Ti, O, and Si in the composite was confirmed and is shown in the (ESI-1‡). The material was further characterized by XPS to examine the elemental composition and oxidation state of elements. The N1s and Si peaks in high-resolution spectrum were centred at 399.95 eV and 101.95 eV, respectively (ESI-3 & 4‡). Further, the binding energy of Ti2p were de-convoluted in two peaks at 458.65 eV and 464.15 eV respectively, which correspond to the spin-orbit coupling of 5.76 eV[35] (ESI-5‡). In addition, the oxygen O1s peak (ESI-2‡) can be de-convoluted into two peaks at 529.95 eV and 532.45 eV, respectively, which show the presence of Ti-O-Ti and Ti-O-Si bonds and thus implying the incorporation of SiO_2 in the TiO_2 matrix[31]. The BET surface area of the N-TiO_2-SiO_2 composite fibers was 36 m^2/g.

The N-TiO_2-SiO_2 composite on reaction with alkali lead to the formation of layered morphology of sodium titanate ($Na_2Ti_3O_7$). The SEM image of the $Na_2Ti_3O_7$ is shown in Fig. 2A. The sheet-like structure of the titanates is evident from the TEM image in Fig. 2B and the inset shows a selected area electron diffraction (SAED) pattern of the $Na_2Ti_3O_7$ which is in good agreement with the XRD pattern. The high-resolution image in Fig. 2C shows the spacing between individual layers of $Na_2Ti_3O_7$ as 0.8 nm[32]. The powder XRD spectrum of titanate . Fig. 2D shows a strong peak around $2\theta=10^o$ confirming the formation of sodium titanate which is the characteristic (100) diffraction peak of the sodium titanates[33]. Elemental mapping was carried out using EDS and the presence of N, Ti, O, Na in composite was confirmed (ESI-6‡). The high-resolution spectra of Ti2p 3/2 and Ti2p ½ are centred at 456.65 and 462.85 eV, respectively, (ESI-7‡), implying that Ti exist in a different chemical environment than that of TiO_2. Further, the binding energy of Na at 1068.7 eV confirms the formation of Ti-O-Na bond[44] (ESI-8‡). The single peak of O1s (ESI-9‡) at 528.25 eV shows the Ti-O-Ti bond[36] and N1s peak been centred at 396.95 eV (ESI-10‡).

Fig. 3A & 3B shows, respectively, the large area and magnified SEM image of sheet-like N-doped 2-D TiO_2 obtained after acidification and low temperature sintering (180^oC) of sodiu titanates. Fig. 3C shows the high-resolution TEM image of N-doped 2-D TiO_2 sheet ranging size from 41-67 nm in breadth and 145-164 nm in length and the inset shows the SAE pattern having discrete rings indicating the polycrystallin nature of the TiO_2. Fig. 3D shows the lattice-resolved TE image of the prepared sample with a lattice spacing of 0.35 n

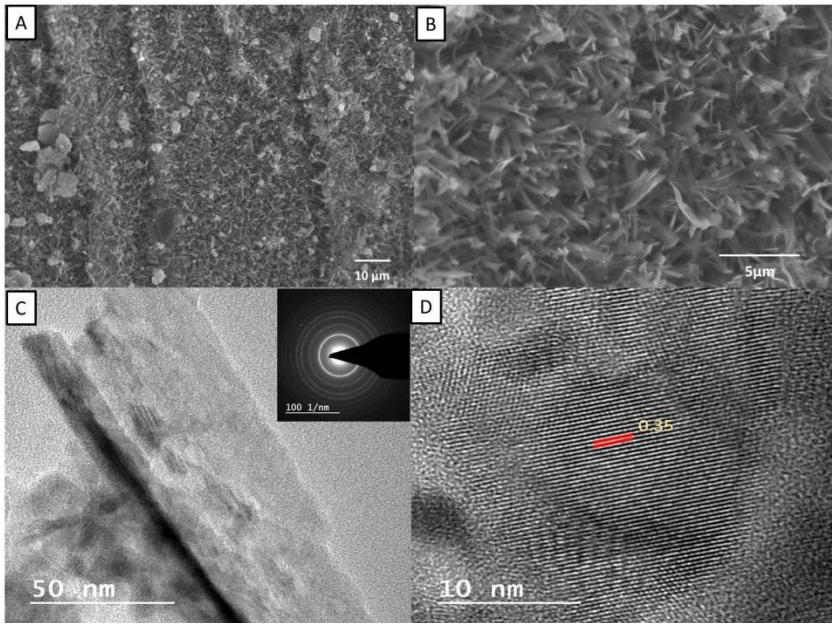

Fig. 3 (A) SEM image of sheet like structure of N-TiO_2 at lower magnification (B) SEM image of sheet like structure of N-TiO_2 at higher magnification (C)HR-TEM mage of N- TiO_2 and the inset SAED(D)Lattice resolved TEM image of N-TiO_2.

which corresponds to the (101) lattice orientation of the anatase TiO_2. A comparison of the SEM and TEM images reveals that the dimensions of the 2-D sheets were in the range of 2-4 µm in length and 278-440 nm in breadth. The UV–Vis diffuse reflectance spectrum (Fig. 4A) was taken for the doped and undoped 2-D TiO_2 annealed at 450 °C and apparently the N-doping has extended the absorbance from UV to the visible region (from 395.33 nm to 412.92 nm, respectively). The band-gap of N doped TiO_2 was calculated (from UV-Vis spectrum) and found to be 3.0 eV. The red-shift in the absorption edge suggests that the increased absorption can be related to the presence of N in the sample. The peaks in the XRD pattern of doped and undoped TiO_2 in Fig. 4B confirms the anatase phase where the prominent peaks shows its crystalline nature which is shown in the spectrum itself and it was found that the peak positions are same and no extra peaks were observed confirming the structure has not changed after the dopant has been added. This might be due to the low amount of nitrogen been doped that cannot be detected by XRD. Further to investigate the effect of N doping on the structure of TiO_2, the Raman spectrum of N- TiO_2 was carried out and the peaks in the Fig. 4C corresponding to 153, 392, 516 and 638 cm^{-1}, respectively, can be attributed to the predominance of anatase phase structure. The Raman peaks at 153 and 638 cm^{-1} represents Eg vibrational mode and the peak at 392 and 516 cm^{-1} corresponds to Bg1 and Ag1 vibrational mode[37]. The Raman shift pattern for doped and undoped TiO_2 was found to be identical and the result indicates that th… nitrogen doping has insignificant effect on the structure of TiO_2. However on comparing the lowest frequency peak at 153 cm^{-1} of un-doped 2-D TiO_2 sheets with N-doped 2-D TiO_2 sheets, it is observed

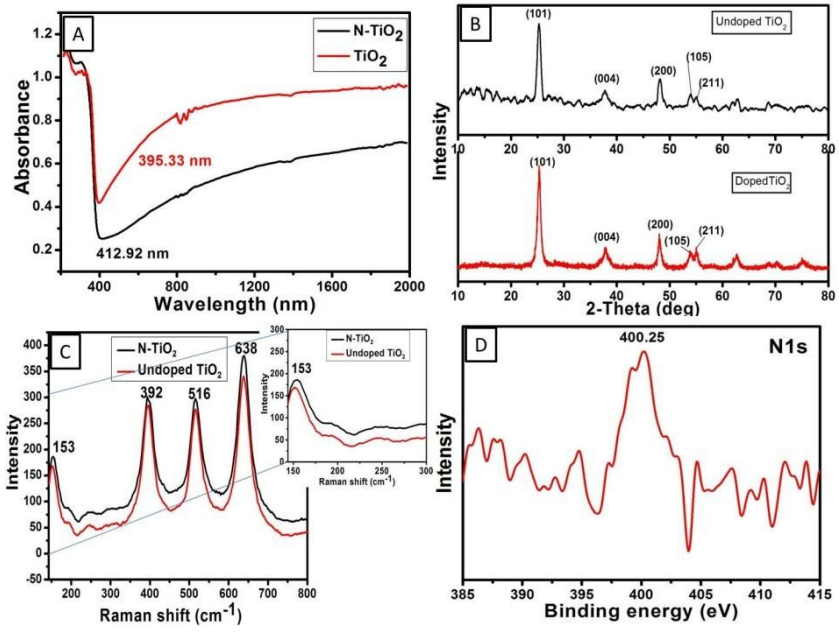

Fig. 4 (A) DRS spectra for N-TiO_2 (B) XRD spectra for doped and undoped TiO_2 (C) Raman spectra for doped and undoped TiO_2(D) XPS spectra for N1s.

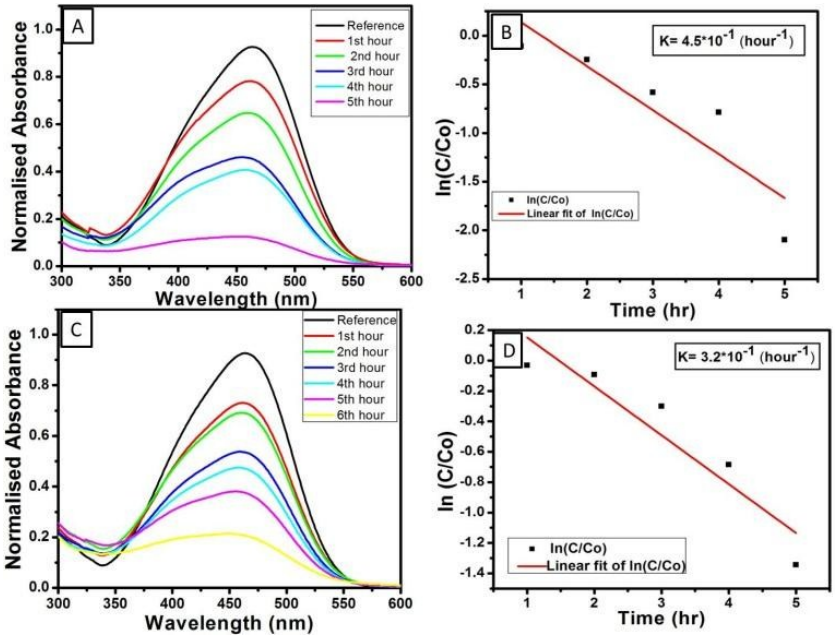

Fig.5(A) Photodegradation of MO by N-doped 2-D TiO_2 sheets (B) rate of reaction for N-TiO_2 2-D sheets (C) photodegradation of MO un-doped TiO_2 2-D sheets (D) rate of reaction of undoped N-TiO_2 2-D sheets.

that the width and the intensity of this peak is increased (Shown in the inset) indicating that the crystallinity has been enhanced after nitrogen doping which is consistent with the XRD results. XPS measurements were carried out in order to confirm the substitution of oxygen atoms by nitrogen in the TiO_2.

From earlier reports[34] it is has been observed that different chemical states have been assigned for N in TiO_2 with varying binding energies ranging from 397ev to 403 eV and the variation in these states strongly depends upon the preparation technique and the precursor used. As per the earlier reports[38,39] the formation of Ti-N bond which is the characteristic of N-doped TiO_2 is centred around 395-397 eV. In addition to it, reports[40,41] on adsorbed NH_3on TiO_2 suggest the characteristic values of binding energy around 398-399 eV. Some reports mention on the presence of NO_x molecules on TiO_2 for which the binding energy value is more than 403 eV[40]. However, Inthe present case, the observed binding energy peak of N1s was at 400.25 eV (Fig. 4D) suggesting the formation of O-Ti-N bond as summarized by Wang et.al[42] with an atomic concentration of 0.34% and has oxidation state of N^{3-}. In the case of Ti2p (ESI-11‡) two peaks were observed at 458.61 and 464.26 eV, respectively, which are attributed to Ti2p3/2 and Ti2p½ indicating that the Ti remains in the octahedral environment. Further Ti2p core levels were compared for doped and undoped samples; we observed that, there were no prominent shifts observed and the peak positions were similar confirming that there is no change in the chemical nature of titanium[43]. Similarly the O1s (ESI-12‡) could be de-convoluted into two peaks, the peak at 529.95 eV corresponds to the Ti-O bond whereas the other peak at 532.45 eV corresponds to the surface hydroxyl groups. The O1s level (ESI 14‡) of doped and undoped sample indicate the presence of O^{2-} attached to Ti^{4+} at 529.95 eV and 529.35 eV respectively[45]. The BET surface area of the N-TiO2 2D sheets was 110 m^2/g.

A model pollutant methyl orange (MO) was selected and the photodegradation of MO (32.72 mg/L) was quantified by measuring its degradation rates under white light in the presence of N–doped 2-D TiO_2 sheets (30 mg). The solution was stirred in dark for 30 min before irradiation to obtain equilibrium of MO on N-doped 2-D TiO_2 sheets. The unabsorbed MO was taken as the initial concentration to estimate the photocatalytic efficiency. Fig. 5A & 5C show the photocatalytic activity of N-doped 2-D TiO_2 and un-doped 2-D TiO_2 indicated by the sequential colour reduction of MO for every 1 h and for the confirmation of photocatalytic activity the absorption spectra was recorded. From Fig. 5B & 5D, it was found that the photocatalytic activity of N-doped 2-D TiO_2 sheets was better having a rate constant of 0.45 (h^{-1}) when compared to undoped 2-D TiO_2 (BET surface area of 104 m^2/g) having a rate constant of 0.32 (h^{-1}). As the doped and undoped TiO_2 were synthesized and processed under similar reaction conditions (as both have nearly same BET surface areas), we believe that the increase in the photocatalytic activity of the N-doped 2-D TiO_2compared to the un-doped TiO_2 resulted mostly from the nitrogen doping.

In conclusion, a highly anisotropic nitrogen-doped 2-D TiO_2 sheets were successfully synthesized from electrospun TiO_2-SiO_2 composite nanofibers. UV-VIS DRS measurements showed the presence of small amount of nitrogen in the catalyst giving rise to a higher visible absorption. The photocatalytic activity of nitrogen-doped 2-D TiO_2 sheet for the degradation

Methyl Orange was compared to undoped TiO_2 2-D sheets. The study showed the N-doped TiO_2 2-D sheets showed an increased photocatalytic activity when compared to undoped TiO_2. Such an improvement in photocatalytic activity is due to the effect of N-doping of TiO_2 which might have introduced additional energy levels in the band-gap thus effectively improving its electronic structure to absorb light in the visible region.

Acknowledgment

The authors acknowledge financial support from the Ministry of New and Renewable Energy (MNRE) and Solar Energy Research Initiative (SERI), Dept. of Science and Technology (DST), respectively, of Govt. of India.

Notes and references

1 D.I. kondarides, Catalysis-Photocatalysis-*Encyclopedia of life support systems*(EOLSS)
2 N. Serpone and A.V. Emeline, *J. Phys. Chem*.,2012,**3**,673-677
3 K. Hashimoto, H. Irie and A. Fujishima, *Jap. J. Appl. Phy., 2005,* **44**,8269-8285
4 B. O'Regan and M. Gr¨atzel, *Nature*, 1991, **353**, 737–740
5 B. Liu, K. Nakata, M. Sakai, H. Saito, T. Ochiai, T. Murakami, K. Takagi and A. Fujishima, *Catal. Sci. Technol*., 2012, **2**, 1933–1939
6 Y. Paza, Z. Luoa, L. Rabenberga and A. Hellera, *J. Mater. Res*., 1995, **10**, 2842-2848.
7 K. GopalMor, A. M. Carvalho, K. O. Varghese, K. M. V. Pishko and A. C. Grimes, *J. Mater. Res*., 2004, **19**, 628-634.
8 (a) Y. Zhou and M. Antonietti, *J. Am. Chem. Soc*., 2003, **125**, 14960 (b) C. M. Lieber and Z. L. Wang, MRS Bull., 2007, **32**, 99-108 (c) T. G. Deepak, G. S. Anjusree, T. Sara,T. A. Arun, S. V. Nair and A. S. Nair, *RSC Adv.,* 2014, **4**, 17615.
9 (a) T. Kasuga, M. Hiramatsu, A. Hoson, T. Sekino and K. Niihara, *Langmuir*, 1998, **14**, 3160; (b) T. Kasuga, M. Hiramatsu, A. Hoson, T. Sekino and K. Niihara, *Adv. Mater*., 1999, **11**, 1307.
10 Y.Qi, Y.Luan, M.Yang, G.Wang, L.Tan, J.Li*, Appl. Surface Sci.,* 2014, **293**,359-365.
11 Q.Li, L.Zong, C.Li, J.Yang, *Appl. Surface Sci., 2014,* **314,** 458-463.
12 A. Pearson, H. Zheng, K. K. Zadeh, S.K. Bhargava, V. Bansal, *Langmuir*, 2012, **28**, 14470-14475
13 T. G. Deepak, G. S. Anjusree, K. R. N. Pai, D. Subash, S. V. Nair and A. S. Nair, *RSC Adv*., 2014, **4**, 27084-27090.
14 Z. Liu, P. Fang, F. Liu, Y. Zhang, X. Liu, D. Lu, D. Li, S. Wang, *Appl. Surface Sci.,* 2014, **305**, 459-465.
15 J. Luo, Q. Chen, X. Dong*, Powder Technol.,* 2015, **275,** 284-289.
16 Q. Xiang, J. Yu, P. K. Wong, *J. colloid interface Sci.,* 2011, 357, 163-167.
17 *K. Ishibashi,* A. Fujishima, T. Watanabe, K. Hashimoto, *Electrochem. Commun.,* 2000, **2,** 207-210.
18 A.Pearson, S.Bhosale, S.K.Bhargava, V.Bansal, *ACS Appl. Mater. Interfaces*, 2013, **5**, 7007-7013.
19 A. Pearson, A. P. O' Mullane, V. Bansal, S. K. Bhargava, *Inorg. Chem.*, 2011, **50**, 1705-1712.
20 M. A. Fox, and M. T. Dulay, *Chem. Rev.*, 1993, **93**, 341-357.
21 H. Kato, and A. Kudo, *J. Phys. Chem.B*, 2002, **106**, 5029-5034.
22 S. Sakthivel, and H. Kisch, *Angew.Chem*, 2003, **42**, 4908-4911.
23 D. G. Huang, S. J. Liao, J. M. Liu, Z. Dang, L. Petrik, *J. Photochem. Photobiol. A*, 2006, **184**, 282-288.
24 C. D. Valentin, G. Pacchioni, *Catal. Today*, 2013, **206**, 12-18.
25 T. Umebayashi, T. Yamaki, H. Itoh, and K. Asai, *J. Phys. Chem. Solids*, 2002, **63**, 1909-1920
26 P. Zhou, J. Yu, Y. Wang*, Applied Catalysis B: Environmental,* 2013*,* **142-143***,* 45-53.
27 R. Ramanathan, V. Bansal, *RSC ADV*, 2015, **5**, 1424-1429.
28 A. Zaleska, Recent patents on engineering, 2008, **2**, 157-164
29 (a) Z. M. Huang, Y. Z. Zhang, M. Kotaki and S. Ramakrishna, *Compos. Sci. Technol.,* 2003, **63**, 2223–2253. (b) D. Li and Y. N. Xia, *Adv. Mater*., 2004, **16**, 1151–1170.
30 I.R.Beattie,T.R.Gilson, *Proc. R. Soc. London*, A, 1968, **307**, 407-429.
31 T. A. Arun, D. K. Chacko, A. A. Madhavan, T. G. Deepak, G. S. Anjusree, T. Sara, S. Ramakrishna, S. V. Nair and A. S. Nair, *RSC Adv*., 2014, **4**, 1421-1424
32 C. Wang, X. Zhang, Y. Zhang, Y. Jia, J. Yang, P.S un and Y. Liu, *J. Phys. Chem. C,* 2011, **115,** 22276-22285
33 K. Kiatkittipong, C. Ye, J. Scott and R. Amal, *Crystal Growth & Design.,* 2010, 8, 3618-3625.
34 B. Viswanathan and K.R. Krishnamurthy, *Intern. J. Photon Energy*, 2012, **2012**, 1-10.
35 A.S. Nair, P. Zhu, V.J. Babu, S. Yang, T. Krishnamoorthy, R. Murugan, S. Peng and S. Ramakrishna, *Langmuir*, 2012, **28**, 6202.
36 A.S. Nair, Z. Peining, V. J. Babu, Y. Shengyuan,Y. Shengjie and S. Ramakrishna,*RSC Adv.*, 2012, **2**, 992
37 C. C. Tsai and H. Teng, *Chem. Mater.*, 2006, **18**, 367.
38 I.Takahashi, D.J Payne, R.G Palgrave, R.G Egdell, *Chem. Phys. Lett.,* 2008, **454,** 314-317.
39 H.Chen, A. Nambu, W. Wen,J.Graciani,Z.Zhong, J.C Hanson, E. Fujita, J.A Rodriguez, *J. Phys. Chem. B.,* 2007, **111**, 1366-1372.
40 J.F. Moulder, W.F Stickle,P.ESobol,K.DBomben.,*Handbook* of X-ray photoelectron Spectroscopy; Eden Prairie: 1992.
41 R.J.J Jansen, H.VanBekkum, *Carbon,* 1995, ***33***, 1021-1027
42 J. Wang, D.N Tafen, J.P Lewis, Z.Hong, A.Manivannan, M.Zhi, M.Li, N.Wu, *J. Am. Chem. Soc.*, 2009,**131**,12290–12297.
43 H. M. Yates, M. G. Nolan, D.W. Sheel, and M. E. Pemble, *J. Photochem. Photobiol. A*, 2006, **179**, 213-223
44 K. Kiatkittipong, C. Ye, J. Scott and R. Amal, *Cryst. Growth Des.*, 2010, **10**, 3618–3625.
45 S. Nandan, T. G. Deepak, S. V. Nair and A. S. Nair, *Dalton Trans.,* 2015, **44**, 9637-9645.